Research Article

Cancer Immunology Research

Glioblastoma Eradication Following Immune Checkpoint Blockade in an Orthotopic, Immunocompetent Model

David A. Reardon[1,2], Prafulla C. Gokhale[3,4], Sarah R. Klein[2], Keith L. Ligon[2,5], Scott J. Rodig[6], Shakti H. Ramkissoon[5], Kristen L. Jones[4], Amy Saur Conway[4], Xiaoyun Liao[2], Jun Zhou[5], Patrick Y. Wen[1], Annick D. Van Den Abbeele[4,7,8], F. Stephen Hodi[2], Lei Qin[4], Nancy E. Kohl[4], Arlene H. Sharpe[9], Glenn Dranoff[2], and Gordon J. Freeman[2]

Abstract

Inhibition of immune checkpoints, including cytotoxic T-lymphocyte antigen-4 (CTLA-4), programmed death-1 (PD-1), and its ligand PD-L1, has demonstrated exciting and durable remissions across a spectrum of malignancies. Combinatorial regimens blocking complementary immune checkpoints further enhance the therapeutic benefit. The activity of these agents for patients with glioblastoma, a generally lethal primary brain tumor associated with significant systemic and microenvironmental immunosuppression, is not known. We therefore systematically evaluated the antitumor efficacy of murine antibodies targeting a broad panel of immune checkpoint molecules, including CTLA-4, PD-1, PD-L1, and PD-L2 when administered as single-agent therapy and in combinatorial regimens against an orthotopic, immunocompetent murine glioblastoma model. In these experiments, we observed long-term tumor-free survival following single-agent anti–PD-1, anti–PD-L1, or anti–CTLA-4 therapy in 50%, 20%, and 15% of treated animals, respectively. Combination therapy of anti–CTLA-4 plus anti–PD-1 cured 75% of the animals, even against advanced, later-stage tumors. In long-term survivors, tumor growth was not seen upon intracranial tumor rechallenge, suggesting that tumor-specific immune memory responses were generated. Inhibitory immune checkpoint blockade quantitatively increased activated $CD8^+$ and natural killer cells and decreased suppressive immune cells in the tumor microenvironment and draining cervical lymph nodes. Our results support prioritizing the clinical evaluation of PD-1, PD-L1, and CTLA-4 single-agent targeted therapy as well as combination therapy of CTLA-4 plus PD-1 blockade for patients with glioblastoma. *Cancer Immunol Res; 4(2); 124–35. ©2015 AACR.*

[1]Center for Neuro-Oncology, Dana-Farber Cancer Institute/Brigham and Women's Hospital, Boston, Massachusetts. [2]Department of Medical Oncology, Dana-Farber Cancer Institute/Brigham and Women's Hospital, Boston, Massachusetts. [3]Belfer Institute for Applied Cancer Science, Dana-Farber Cancer Institute/Brigham and Women's Hospital, Boston, Massachusetts. [4]Lurie Family Imaging Center, Dana-Farber Cancer Institute/Brigham and Women's Hospital, Boston, Massachusetts. [5]Center for Molecular Oncologic Pathology, Dana-Farber Cancer Institute/Brigham and Women's Hospital, Boston, Massachusetts. [6]Department of Pathology, Brigham and Women's Hospital, Boston, Massachusetts. [7]Department of Imaging, Dana-Farber Cancer Institute, Boston, Massachusetts. [8]Department of Radiology, Brigham and Women's Hospital, Boston, Massachusetts. [9]Department of Microbiology and Immunobiology, Harvard Medical School, Boston, Massachusetts.

Note: Supplementary data for this article are available at Cancer Immunology Research Online (http://cancerimmunolres.aacrjournals.org/).

P.C. Gokhale and S.R. Klein contributed equally to this article.

Current address for N.E. Kohl: Blueprint Medicines, 38 Sidney Street, Cambridge, MA 02139; and current address for G. Dranoff, Novartis Institutes for BioMedical Research, 250 Massachusetts Avenue, Cambridge, MA 02139

Prior Presentation: Presented in part at the 50th Annual Meeting of the American Society of Clinical Oncology, 2014, and the 19th Annual Meeting of the Society for Neuro-Oncology, 2014.

Corresponding Author: David A. Reardon, Dana-Farber Cancer Institute, 450 Brookline Avenue, Dana 2134, Boston, MA 02215. Phone: 617-632-2166; Fax: 617-632-4773; E-mail: david_reardon@dfci.harvard.edu

doi: 10.1158/2326-6066.CIR-15-0151

Introduction

Outcomes for glioblastoma, the most aggressive primary cancer of the brain, remain dismal. The most effective chemotherapeutic, the alkylating agent temozolomide, extends survival by a modest 2.5 months and results in a median survival of 14.6 months (1, 2). In addition, recently reported phase III clinical trials evaluating chemotherapy dose intensification (3), antiangiogenic therapy (1, 2), and integrin inhibition (3) have failed to improve survival. Innovative treatment strategies to improve outcome for this unmet patient need remain imperative.

Historical dogma purporting immunoprivilege of the central nervous system (CNS) has gradually eroded, with the demonstration of lymphatics within the CNS (4) and growing data supporting a dynamic interaction between the CNS and the systemic immune systems (5). This paradigm shift has contributed to a growing interest in the evaluation of immunotherapeutic approaches for brain tumors, including glioblastoma. A variety of vaccination strategies have demonstrated encouraging preliminary results (9). Nonetheless, the dominant immunosuppressive mechanisms exploited by glioblastoma tumors to resist antitumor immune attack likely limit improvement in outcomes.

Immune checkpoints normally function to reduce or abrogate immune system responses to specific antigens. Among inhibitory checkpoints, cytotoxic T-lymphocyte antigen-4 (CTLA-4) and programmed death-1 (PD-1) expression markedly increases upon T-cell activation (6, 7). CTLA-4 reduces early stages of T-cell

expansion primarily in systemic lymph nodes by out-competing CD28 for B7-ligand binding (8). In contrast, PD-1 interacts with its ligands PD-L1 and PD-L2 to inhibit T-cell receptor–dependent proliferation and cytokine production, alter T-cell motility and metabolism, and enhance survival of regulatory T cells (Treg) primarily within peripheral lymph nodes and regions of inflammation (6, 9, 10). CTLA-4 and PD-1 normally serve as nonredundant, serial, negative regulators to protect normal tissues from damage associated with immune system activation and to foster immunotolerance to prevent autoimmunity.

Many tumors exploit the normally protective role of inhibitory immune checkpoints as a strategy to evade immune system attack. Tumor-infiltrating lymphocytes can express large amounts of PD-1, which may reflect an exhausted phenotype including poor effector function and enhanced expression of other inhibitory receptors (6, 7). PD-L1 and PD-L2 are also expressed by many tumors and in some series have been linked with poor prognosis (8, 9). Among glioblastoma tumors, nearly 90% diffusely express PD-L1 (6), expression of which is linked with loss of the PTEN tumor-suppressor gene, which occurs in up to 40% of glioblastoma tumors (11, 12).

Individual blockade of CTLA-4, PD-1, or PD-L1 has achieved noteworthy benefit for patients with challenging solid tumors and lymphoid malignancies, including durable tumor regression in up to 25% of patients with advanced melanoma (13–15), and combined blockade of CTLA-4 and PD-1 increased the response rate to approximately 70% in the same population (16). The therapeutic benefit associated with these agents for patients with glioblastoma has not been determined, and limited preclinical glioblastoma data reveal variable results. We therefore conducted a systematic evaluation with blocking CTLA-4, PD-1, PD-L1, and PD-L2 mAbs against an orthotopic, immunocompetent GL261 glioblastoma model. In addition to separate blockade of each individual checkpoint, we also evaluated combinatorial regimens with potentially complementary mechanisms of activity. Given the nonredundant regulatory roles of CTLA-4 and PD-1 signaling on T-cell activity, and the documented enhanced antitumor effect of combined blockade observed in patients (7), we first evaluated blockade of CTLA-4 with inhibition of either PD-1 or PD-L1. We then evaluated PD-1 blockade with inhibition of either PD-L1 or PD-L2 as a strategy to more effectively suppress overall PD-1–mediated immunosuppression in this model.

Our results reveal that blockade of CTLA-4, PD-1, or PD-L1 alone can eradicate growing glioblastoma tumors within the CNS, including late-stage tumors. Antitumor activity can be augmented by combinatorial therapy targeting CTLA-4 and PD-1. We also noted that long-term survivors show immune memory responses capable of preventing tumor growth following rechallenge. Finally, we demonstrate that combined CTLA-4 and PD-1 blockade enhances infiltration of effector immune cells while reducing suppressive immune cell subsets within the tumor microenvironment and draining cervical lymph nodes.

Materials and Methods

Cell line, antibodies, and reagents

Luciferase-transduced GL261 cells (GL261-luc2) were purchased (Perkin-Elmer) in 2014, expanded, and frozen without further testing or authentication. Thawed cells were cultured for up to three passages in DMEM supplemented with 10% heat-inactivated FCS and 100 μg/mL G418 at 37°C in a humidified incubator maintained at 5% CO_2 prior to intracranial implantation. Cells were maintained in logarithmic growth phase for all experiments.

The following mouse anti-mouse mAbs were generated in specific gene-deficient mice, in the laboratory of Dr. Gordon Freeman: PD-1 – 332.8H3 (mouse IgG1, K); PD-L1 – 339.6A2 (mouse IgG1, K), and PD-L2 – 3.2 (mouse IgG1, K; ref. 7). Mouse anti-mouse CTLA-4 – 9D9 (mouse IgG2b, K) was purchased from BioXCell. Each of these mAbs blocks interaction with ligand. Isotype controls were purchased from BioXCell and included MOPC21 (IgG1), MPC-11 (IgG2b), and C1.18 (IgG2a). All mAbs contained less than 2 endotoxin units/mg protein.

Intracranial tumor cell inoculation

GL261-luc2 cells (1×10^5), which are syngeneic in C57BL/6 mice (8), were resuspended in PBS and injected stereotactically into the right striatum of anesthetized, 6- to 10-week-old female albino C57BL/6 mice (The Jackson Laboratory) using a Hamilton syringe and stereotactic frame. Mice were euthanized for signs of morbidity due to tumor burden or 120 days after reinjection if they appeared to be healthy. All animal experiments were approved by the Dana-Farber Animal Care and Use Committee.

In vivo treatment and tumor assessment

For all studies, mice with enlarging tumor burden defined by increasing bioluminescence signal between days 3 and 6 after tumor implantation were randomized into control and treatment cohorts (8 mice per cohort). Tumor response assessment was done by quantifying bioluminescence in all animals as well as MRI imaging in a subset (see Supplementary Materials and Methods).

First, we determined the antitumor effect against a growing, established tumor model. Therapeutic mAbs and isotype controls were administered via intraperitoneal injection beginning on day 6 (500 μg) after tumor implantation with repeat injections every 3 days (250 μg/dose) for a total of eight injections. Control animals received equivalent doses of isotype murine IgG according to the same dosing schedule. No treatment was administered after day 27 following tumor implantation. Using this treatment schedule, we systematically evaluated the antitumor activity as measured by survival using mAbs against CTLA-4, PD-1, PD-L1, and PD-L2 as single agents and in combinatorial regimens in separate experiments.

We then addressed whether inhibitory immune checkpoint blockade can have a therapeutic effect against an advanced, later-stage tumor model. A similar treatment schema to that detailed above was employed, but treatment was initiated on day 14 after tumor implantation. CTLA-4 or PD-1 mAb monotherapy or in combination, as well as appropriate isotype controls, were repeated every 3 days for eight total doses. No further therapy was administered beyond day 35 after tumor implantation.

Rechallenge experiments

GL261-luc2 cells (1×10^5) were injected intracranially into the contralateral hemisphere in a cohort of mice previously treated beginning on day 6 who survived over 100 days as well as 5 treatment-naïve CL57BL/6 albino mice. Rechallenged mice were followed for a minimum of 100 additional days and received no additional therapy. Mice were then sacrificed, at which point the brain was removed, fixed in 4% formalin, and embedded in paraffin. Two 3-μm sections were stained with hematoxylin and eosin and then examined for microscopic evidence of tumor by

two neuropathologists (K.L. Ligon and S.H. Ramkissoon) blinded to prior treatment.

Characterization of immune response

Immune response assessment studies were performed on material obtained from euthanized, tumor-bearing animals on day 24 following mAb treatment administered on days 14, 17, 20, and 23. For flow cytometry, brains, spleens, and superficial cervical lymph nodes were harvested and homogenized using enzymatic (1.5 mg/mL collagenase IV, 200 U/mL DNaseI, HBSS with calcium and magnesium) and/or mechanical tissue disaggregation. Brain cells were resuspended in 25% Percoll Plus (Sigma) for myelin removal and leukocyte isolation. Red blood cells were removed using a Ficoll gradient (GE Life Sciences). The following antibodies were used for flow cytometric analysis of cell surface proteins: anti-CD45 (30-F11; Biolegend), anti-CD3 (17A2; Biolegend), anti-CD4 (RM4-5; Biolegend), anti-CD8 (53-6.7; Biolegend), anti-CD11b (M1/70; Biolegend), anti-CD86 (GL-1; Biolegend), anti-NK1.1 (PK136; Biolegend), anti-Gr1 (RB6-8C5; Biolegend), anti-PD1 (RMP1-30; eBioscience), anti-Tim3 (B8.2.C12; Biolegend), and anti-CTLA4 (UC10-4B9; Biolegend). Dead cells were excluded using the Zombie NIR Fixable Viability Kit (Biolegend). Following surface staining, cells were fixed and permeabilized with the FoxP3 Fixation/Permeabilization Kit (eBioscience). The following antibodies were used for intracellular staining: anti-FoxP3 (MF-14; Biolegend) and anti-Granzyme B (NGZB; eBioscience). Acquisition was performed on an LSR Fortessa SORP HTS flow cytometer (BD Biosciences). Data analysis was performed using FlowJo X 10.7.7r2 (Tree Star).

Immunohistochemistry studies for the detection of CD4- and CD8-positive lymphocytes were performed on separate, snap-frozen, and paraffin-embedded portions of the frontal cerebrum according to the established methods. Analysis of circulating immunocytokines was performed on serum using the Mouse Chemokine Antibody Array (R&D Systems) according to the manufacturer's instruction (for further details, see Supplementary Materials and Methods).

Statistical analysis

Survival estimates and median survivals were determined using the method of Kaplan and Meier. A log-rank (Mantel–Cox) test was used to calculate *P* values derived from statistical analysis of Kaplan–Meier survival curves. A one-way ANOVA followed by a Tukey multiple comparisons test was used to determine the statistical significance between two experimental groups in the flow cytometric and serum analysis. *P* values of less than 0.05 were considered statistically significant (*, $P < 0.05$; **, $P < 0.01$; ***, $P < 0.001$). Quantitative analysis was performed with Graphpad Prism 6 (Graphpad Software, Inc.).

Results

Eradicating established glioblastoma tumors and generating long-term survival

We first performed a series of experiments to systematically evaluate the antitumor activity of blocking individual inhibitory immune checkpoint molecules as well as combinatorial regimens with potentially complementary mechanisms of action (Fig. 1 and Table 1). In our initial experiments, treatment began on day 6 against an established, growing model tumor, GL261-luc2 (Fig. 1A). Intracranial bioluminescence of all animals initially increased for 1 to 2 weeks, consistent with growing tumor burden. Thereafter, bioluminescence decreased in responding mice, consistent with tumor regression. In contrast, nonresponders in each treatment cohort progressively increased luciferase counts (Fig. 2 and Supplementary Fig. S1). Changes in tumor burden were confirmed by MRI in a subset of treated mice (Fig. 2).

Using the established tumor model, we compared blockade of CTLA-4, PD-1, and PD-L1 separately (Fig. 1B and C). PD-1 blockade showed the greatest efficacy, with long-term effective cures in 56% of the treated animals, whereas blockade of either PD-L1 or CTLA-4 had less survival benefit. Because CTLA-4 and PD-1 suppress T-cell activation nonredundantly, we also evaluated the antitumor effect of CTLA-4 blockade with either PD-1 mAb or PD-L1 mAb. In these experiments, CTLA-4 mAb combined with PD-1 mAb led to an effective cure rate of 75% (Fig. 1B). In contrast, the addition of PD-L1 blockade to CTLA-4 mAb had a negligible effect (Fig. 1C).

We also compared and combined blockade of PD-1, PD-L1, and PD-L2 and found that PD-1 mAb improved survival better than PD-L1 mAb, whereas PD-L2 mAb had no effect (Fig. 1D and E). Of note, combinatorial therapy with PD-1, PD-L1, or PD-L2 did not improve survival compared with single-agent PD-1 or PD-L1 mAb therapy.

Of note, long-term ($\geq$100 days) survivors were observed in a subset of mice treated with PD-1, CTLA-4, and PD-L1 mAbs, as well as combinations thereof (Fig. 1B–E and Table 1). These animals appeared healthy and neurologically intact. In addition, there was no evidence of intracranial tumor noted upon histopathologic examination in this subset (data not shown). The median survival of mice treated with any immune checkpoint mAb except anti–PD-L2, as well as combinations thereof, was longer than that of control mice (Table 1). Among cohorts of mice treated with single-agent therapy, median survival was longest among PD-1 mAb–treated mice (91 days). Among mice treated with combination therapy, PD-1 mAb plus CTLA-4 mAb increased survival additively when compared with single-agent therapy. This combination achieved the longest survival (median not reached at 141 days, at which point survivors were euthanized) of any treatment cohort in our experiments. In contrast, median survival of the other combination groups was modestly improved compared with that of controls, but did not differ significantly from mice treated with single-agent therapy.

Immunologic memory that prevents recurrence following tumor rechallenge

To examine the development of immunologic memory, long-term (>100 days) survivors of checkpoint therapy for established tumors were challenged with contralateral intracranial injection of 1×10^5 GL261-luc2 cells (Fig. 3A). Thirteen of 14 (93%) long-term survivors following mAbs against PD-1 ($n = 5$), CTLA-4 ($n = 3$), or combination PD-1+ CTLA-4 ($n = 6$) therapy survived after rechallenge for an additional 120 days (Fig. 3B). When sacrificed, these mice showed no evidence of microscopic intracranial tumor (Fig. 3C). In contrast, 4 of 5 treatment-naïve control mice died approximately 30 days following injection of GL261-luc2 cells.

Advanced, later-stage glioblastoma tumors effectively treated with immune checkpoint blockade

In order to evaluate the therapeutic impact of immune checkpoint blockade against an advanced intracranial glioblastoma tumor model, we initiated treatment on day 14 after tumor

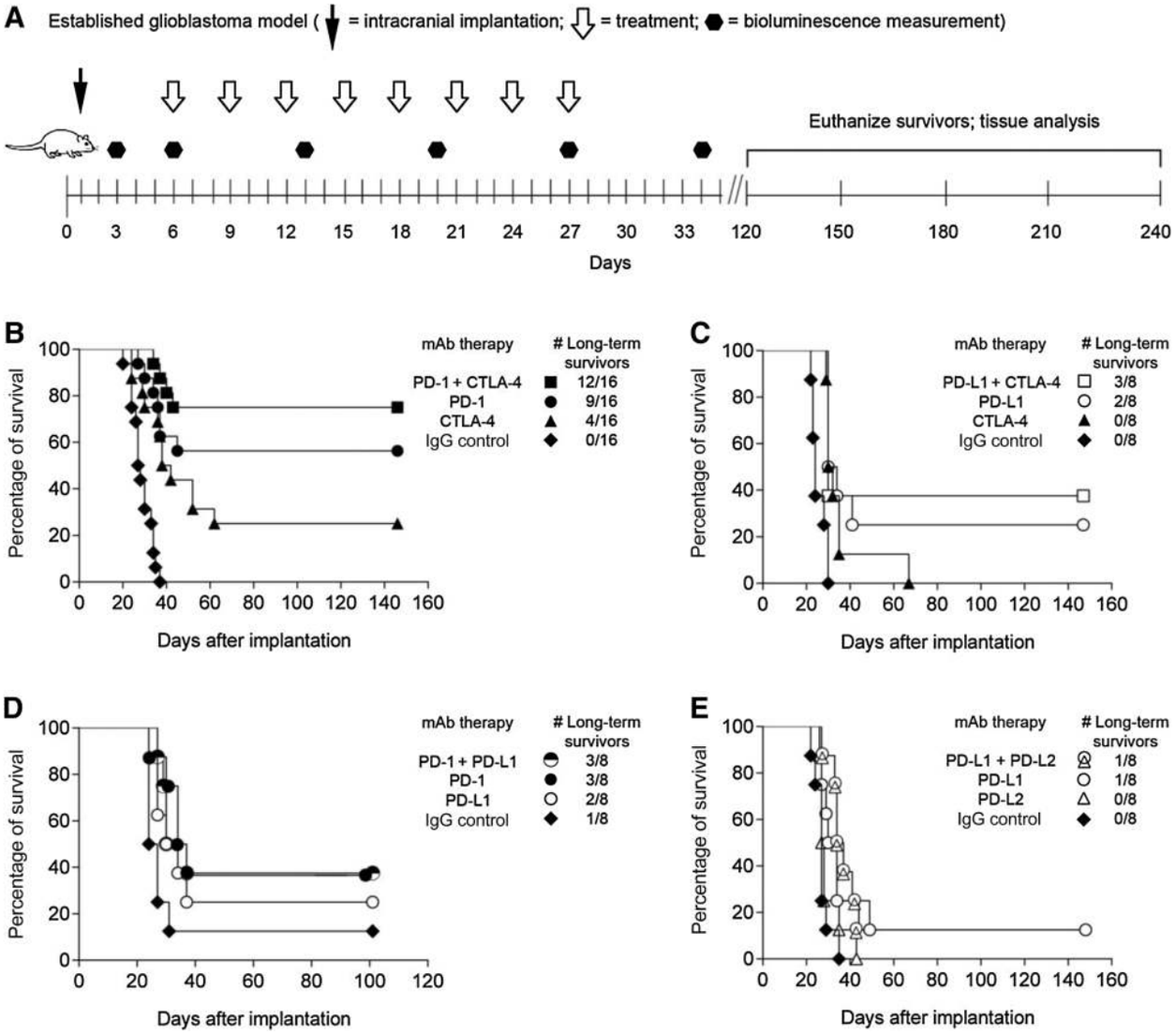

Figure 1.

Immune checkpoint blockade improves survival against an established intracranial GL261-luc2 (1×10^5 cells) glioblastoma tumor model including long-term tumor-free survival (A). Monitoring and treatment schema and Kaplan–Meier survival curves following immune checkpoint blockade using mAbs against CTLA-4 and PD-1 (B), CTLA-4 and PD-L1 (C), PD-1 and PD-L1 (D), and PD-L1 and PD-L2 (E). Each experiment includes 8 mice per cohort and IgG isotype controls.

implantation (Fig. 4A). By day 14, tumors were readily detectable by MRI (data not shown). Treatment was repeated every 3 days for eight total doses with no further therapy administered after day 35 following tumor implantation. As expected, control animals died from progressive tumor within 28 to 30 days. In contrast, 1 of 8, 4 of 8, and 7 of 8 animals, which were treated with mAbs to CTLA-4, PD-1, or CTLA-4 plus PD-1, respectively, remained alive without evidence of tumor or neurologic compromise >100 days following tumor implantation (Fig. 4B).

Intratumoral analysis: enhanced immune effector cell infiltration while decreasing immunosuppressive cells

We evaluated changes in intratumoral and systemic immune cell subsets in mice treated with mAbs against CTLA-4, PD-1, or combination CTLA-4 plus PD-1 compared with isotype control antibody. In these studies, treatment of advanced disease was initiated on day 14 after tumor implantation as depicted in Fig. 4 and repeated on days 17, 20, and 23 prior to sacrificing the animals on day 24.

Flow cytometry analysis of tumor-infiltrating immune cells (Figs. 5 and 6 and Supplementary Fig. S2) revealed an increased number of $CD8^+$ cytotoxic T cells and decreased number of $CD4^+$ $FoxP3^+$ Tregs that reached statistical significance for mice treated with CTLA-4 mAb plus PD-1 mAb combination therapy compared with controls (Fig. 5A and B). Single-agent CTLA-4 and PD-1 mAb therapy was also associated with a significant reduction of tumor-infiltrating Tregs (Fig. 5B). In accordance with these data, the $CD8^+$ effector cell/$CD4^+FoxP3^+$ Treg ratio was significantly increased for the combination therapy cohort compared with controls (Fig. 5C). We also noted a statistically significant

Table 1. Outcome by treatment cohort for individual (A) and aggregate (B) experiments against an established glioblastoma model

	Figure	Treatment mAb	# Treated	Number of long-term survivors (% of cohort)	Median survival (days)	*P* value[a]
A	1B	Isotype control	16	0	27.5	NA
		CTLA-4	16	4 (25)	40.0	<0.0001
		PD-1	16	9 (56.3)	>146	<0.0001
		CTLA-4 + PD-1	16	12 (75)	>146	<0.0001
	1C	Isotype control	8	0	24.0	NA
		CTLA-4	8	0	31.0	0.0025
		PD-L1	8	2 (25)	32.0	0.0012
		CTLA-4 + PD-L1	8	3 (37.5)	30.0	0.0016
	1D	Isotype control	8	1 (12.5)	25.5	NA
		PD-1	8	3 (37.5)	35.5	0.049
		PD-L1	8	2 (25)	32.0	NS
		PD-1 + PD-L1	8	3 (37.5)	33.5	NS
	1E	Isotype control	8	0	27.0	NA
		PD-L1	8	1 (12.5)	32.0	0.045
		PD-L2	8	0	27.5	NS
		PD-L1 + PD-L2	8	1 (12.5	35.5	0.004
B	1B, 1C, 1D, and 1E	Isotype controls	40	1 (2.5)	27.0	NA
	1B and 1C	CTLA-4	24	4 (16.6)	36.5	<0.0001
	1B and 1D	PD-1	24	12 (50)	96.5	<0.0001
	1C, 1D, and 1E	PD-L1	24	5 (20.8)	32.0	0.0003
	1E	PD-L2	8	0	27.5	NS
	1B	CTLA-4 + PD-1	16	12 (75)	>146	<0.0001
	1C	CTLA-4 + PD-L1	8	3 (37.5)	30.0	0.0016
	1D	PD-1 + PD-L1	8	3 (37.5)	33.5	NS
	1E	PD-L1 + PD-L2	8	1 (12.5)	35.5	0.004

Abbreviations: NA, not applicable; NS, not statistically significant.
[a]*P* value reflects comparison with isotype control cohort.

increase of intratumoral activated natural killer (NK) cells (percent CD86$^+$ gated on NK1.1$^+$ cells; refs. 9, 10) compared with controls for each treatment cohort (Fig. 5D).

In addition, we characterized tumor-infiltrating T cells (TIL) for expression of immunoinhibitory receptors CTLA-4, PD-1, or PD-1 and TIM-3 coexpression (PD-1$^+$/TIM3$^+$). The latter represents a particularly exhausted CD8$^+$ T-cell population within tumors (11, 12). Although CTLA-4–expressing TILs were comparable among treatment groups and controls (data not shown), the numbers of PD-1–positive (Fig. 6A and B) and PD-1$^+$/TIM3$^+$ TILs

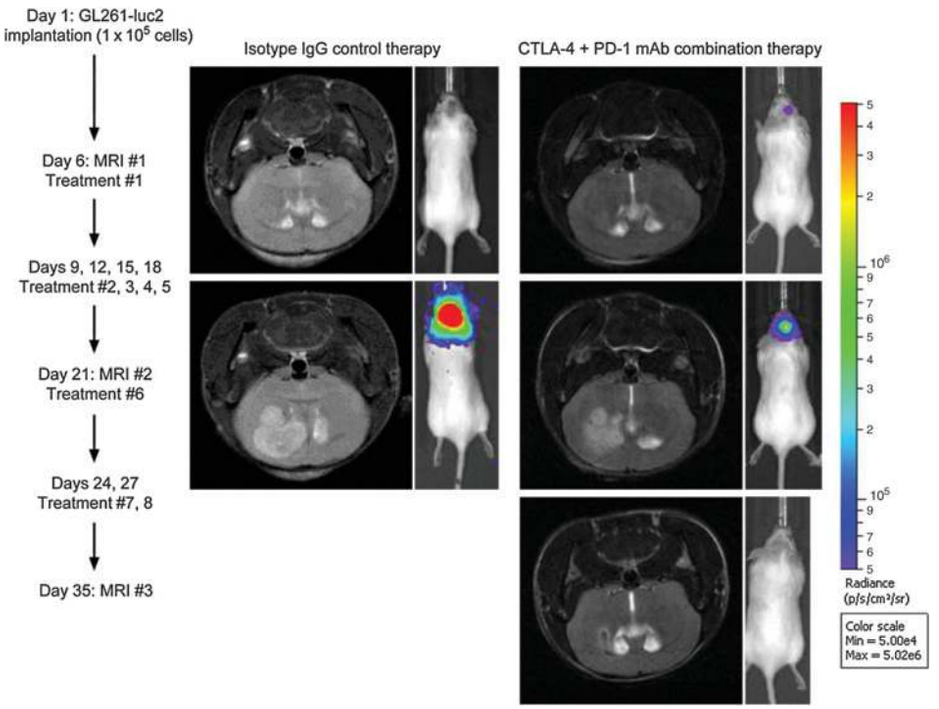

Figure 2.
Regression of growing GL261-luc2 tumors following inhibitory immune checkpoint blockade. Representative MRI findings and bioluminescence of a control mouse treated with isotype control IgG and a responding mouse treated with CTLA-4 plus PD-1 mAb therapy. Following intracranial implantation of GL261-luc2 cells on day 0 (1×10^5 cells), mice were treated on days 6, 9, 12, 15, 18, 21, 24, and 27. MRI scans were obtained on days 6, 21, and 35 along with bioluminescence quantitation. On day 21 mice treated with isotype control IgG as well as those treated with CTLA-4 plus PD-1 combination mAb therapy had increased T2WI signal abnormality and increased bioluminescence counts consistent with tumor growth. Control animals died from progressive tumor by day 30 and therefore did not have repeat imaging on day 35. Animals responding to combinatorial immune checkpoint blockade had decreased size of FLAIR signal abnormality on MRI and loss of fluorescence signal consistent with regressing tumors.

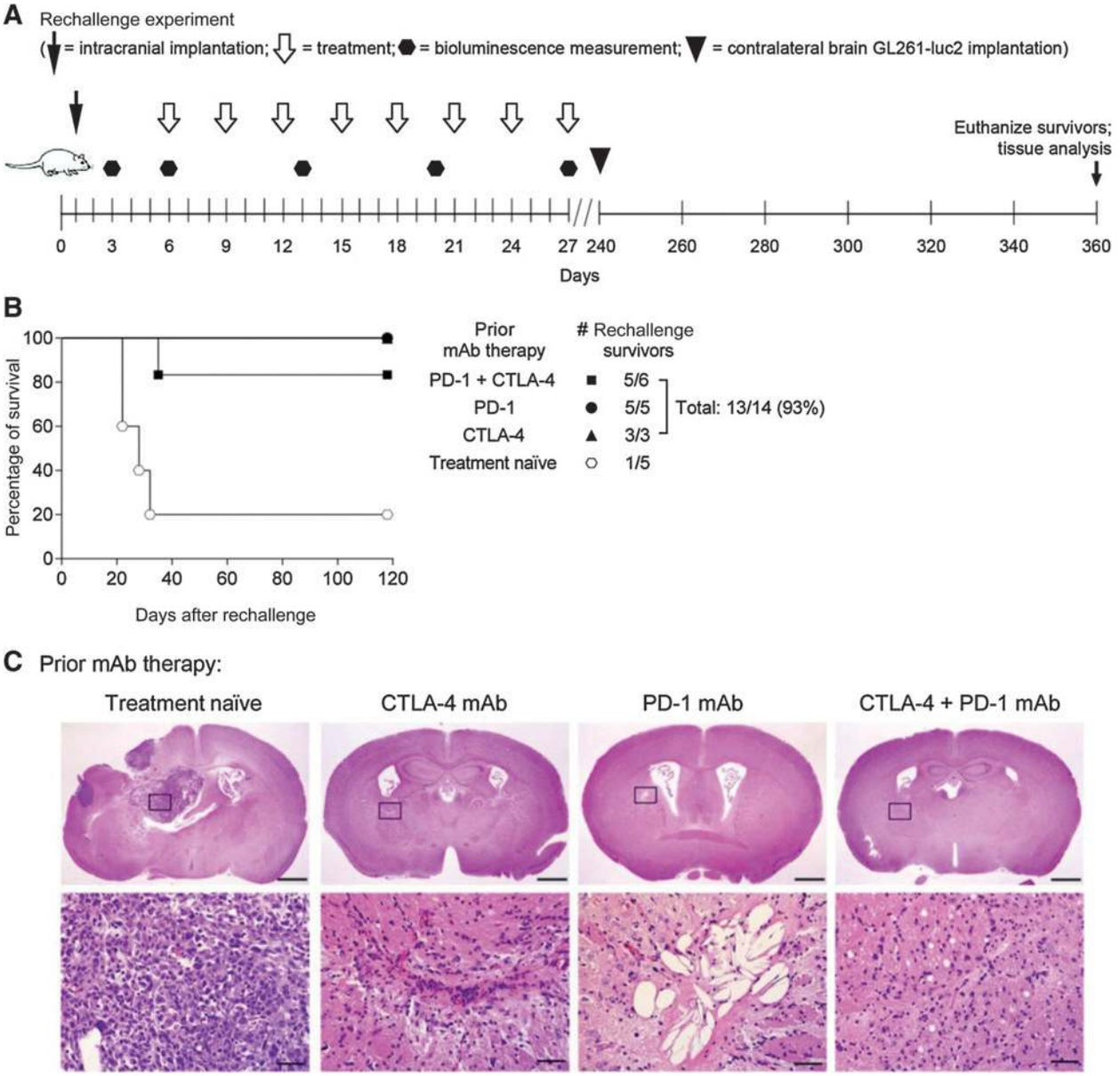

Figure 3.
Checkpoint blockade survivors reject intracranial tumor rechallenge consistent with antitumor memory immune responses. A, monitoring and treatment schema. B, Kaplan–Meier survival curves of long-term survivors (>100 days) initially treated with the indicated mAbs or treatment-naïve controls following intracranial inoculation of 1×10^5 GL261-luc2 cells. No treatment was given after tumor rechallenge. C, histopathologic examination of postmortem brains of rechallenged mice and treatment-naïve controls. Representative images from long-term ($\geq$ 100 days) survivors after rechallenge reveal some small focal areas of chronic vacuolated parenchymal injury and macrophage immune cell infiltrate at site of initial tumor implantation but no residual tumor.

(Fig. 6C) were markedly lower among mice treated with either PD-1 or CTLA-4 plus PD-1 mAbs compared with controls. Of note, the PD-1 staining mAb used is not blocked by the PD-1 treatment mAb and does not share the same epitope (Supplementary Fig. S3). Moreover, myeloid-derived suppressor cells (MDSC; $CD11b^+Gr1^+$) in tumors showed a downward trend for each treatment cohort but only achieved statistical significance for the combination cohort compared with controls (Fig. 6D). Immunohistochemical analysis confirmed enhanced CD4 and CD8 infiltrates in general, which were most striking following combination PD-1 plus CTLA-4 mAb therapy (Supplementary Fig. S4).

Systemic immune system changes induced by immune checkpoint blockade

Changes in lymphocyte subsets in draining cervical lymph nodes followed similar trends as observed among TILs (Figs. 5 and 6 and Supplementary Fig. S5). Specifically, cytotoxic $CD8^+$

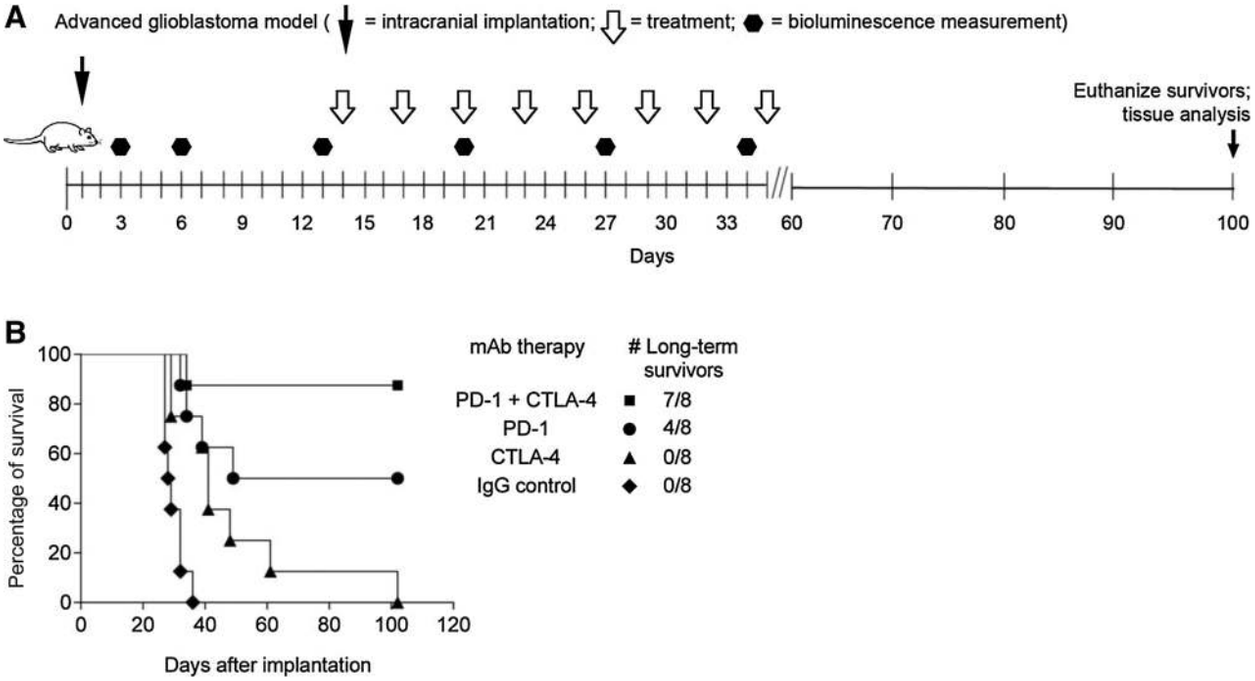

Figure 4.
Immune checkpoint blockade improves survival against an advanced, later-stage intracranial GL261-luc2 glioblastoma tumor model including long-term tumor-free survival. A, monitoring and treatment schema for advanced disease model. B, Kaplan–Meier survival curves following inhibitory immune checkpoint blockade using mAbs against CTLA-4 and PD-1.

and CD8/Treg ratios were increased, whereas FoxP3$^+$ Tregs and PD-1$^+$/TIM3$^+$ lymphocytes were decreased among combination-treated animals compared with controls. In contrast, lymphocytes isolated from the spleens of CTLA-4–treated and combination-treated mice had higher percentages of Tregs and PD-1$^+$/Tim3$^+$ T cells (Figs. 5 and 6).

Activated NK cells were increased in both the cervical lymph nodes and spleens among mice receiving checkpoint blockade in a pattern similar to that observed in tumors (Fig. 5D). In contrast, MDSCs decreased in the tumor but increased in both cervical lymph nodes and spleens of treated animals (Fig. 6D). The significance of changes observed systemically versus only in the tumor requires further investigation.

We also evaluated the effect of immune checkpoint blockade on serum concentration of 24 chemokines in our model of advanced glioblastoma (Supplementary Fig. S6 and Supplementary Table S1). We detected significant increases in chemokines CCL9 (MIP-1γ), CCL6 (C10), CCL11 (eotaxin), CXCL12 (SDF-1), and CCL8 (MCP-2) in the serum of single-agent–and/or combination-treated animals. Changes in other evaluated chemokines did not achieve statistical significance.

Discussion

Therapeutics targeting immune checkpoint mediators, such as CTLA-4 and PD-1, have achieved profound benefit across a growing number of cancer indications, yet their value for patients with glioblastoma, the most common and deadliest CNS malignancy, remains unknown. Furthermore, preclinical studies to date vary significantly with regard to methods and reagents, leading in turn to a wide spectrum of outcome and uncertain conclusions. We therefore performed a series of experiments that incorporated novel and strategic considerations in order to clarify the potential value of inhibitors targeting CTLA-4 and PD-1 signaling for glioblastoma.

As a first step, we utilized immune checkpoint–blocking mAbs that accurately reflect reagents currently used in the clinic for patients. Current clinical efforts to inhibit CTLA-4 among cancer patients use a human mAb that blocks interaction with B7 ligands and has an Fc that can enlist antibody-dependent cytotoxicity (ADCC) to deplete CTLA-4–expressing Tregs (13). In contrast, currently approved human PD-1 mAbs are designed to block interaction with ligands, but have an Fc that does not enlist ADCC (13). To best model this effect in mice, we used mouse CTLA-4 and PD-1 antibodies with the same properties to treat orthotopic, intracranial glioblastoma tumors in immunocompetent mice. This strategy contrasts with most preclinical experiments including those previously reported for glioblastoma (14–19), which use rat or hamster antibodies in mice and are limited in duration by the development of mouse anti-rat antibodies. Notably, the use of syngeneic mouse mAbs in our study should reduce anti-antibody responses, allow for longer treatment, and more closely model the human clinical experience. Among the immune checkpoints targeted in our experiments, only PD-L1 was detectable on GL-261 cells (Supplementary Fig. S7), indicating that the observed therapeutic benefit of PD-1 and CTLA-4 mAbs was due primarily to effects on immune cells rather than the tumor itself.

Second, in order to assess which single-agent and combination targets provide the greatest antitumor benefit, we systematically blocked CTLA-4 components of PD-1 signaling, including PD-1,

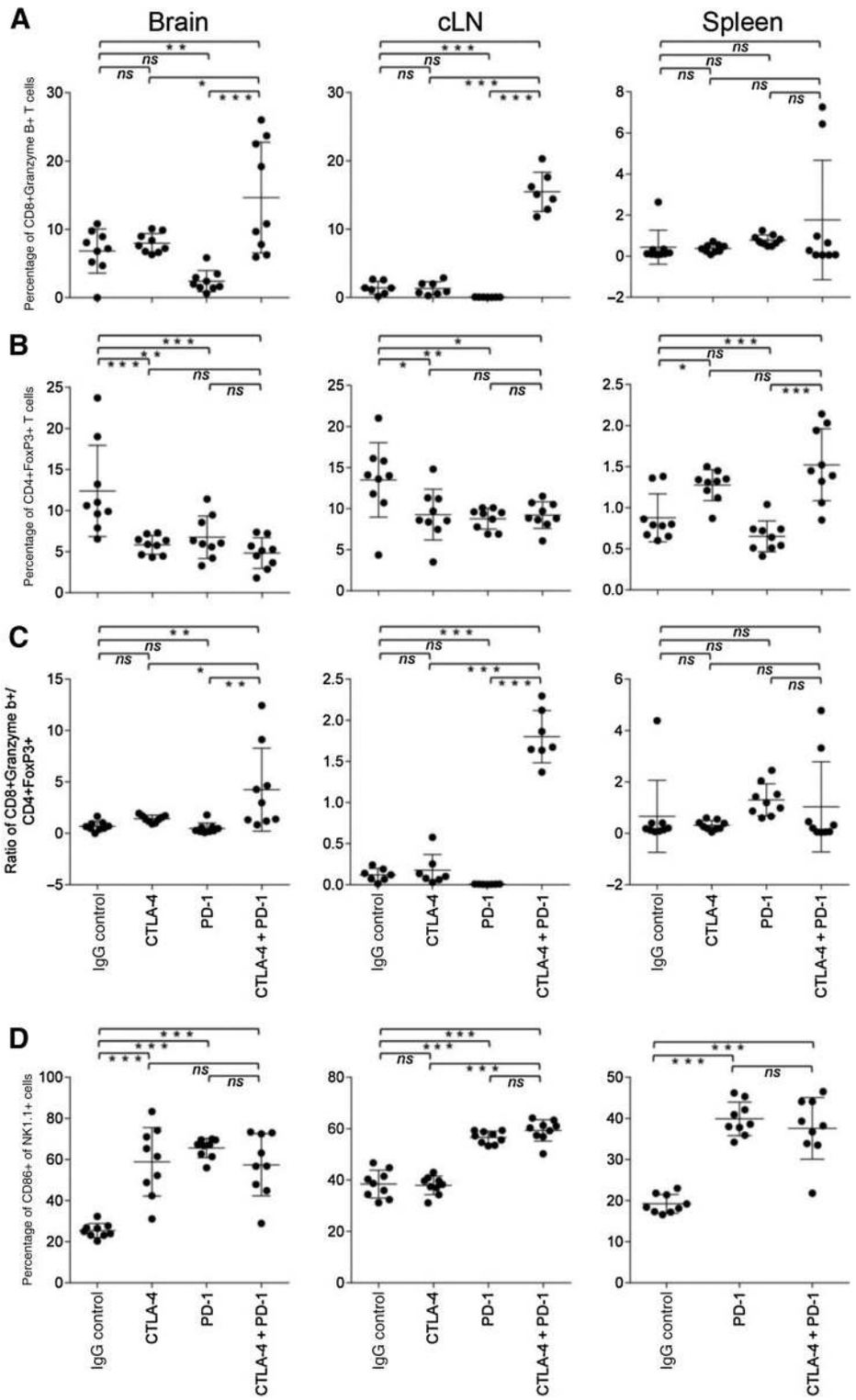

Figure 5.
Immune cell infiltrates within intracranial tumor, draining cervical lymph nodes (cLN), and spleen following checkpoint blockade. Tumor was established with advanced disease and treated as shown in Fig. 4 with isotype control IgG or mAbs against CTLA-4, PD-1, or the combination of CTLA-4 plus PD-1. Leukocyte populations were prepared from tissues on day 24. A, $CD8^+$/granzyme B^+ effector T cells as a percentage of live $CD45^+CD3^+$ cells. B, $CD4^+$/$FoxP3^+$ Tregs as a percentage of live $CD45^+CD3^+$ cells. C, the ratio of effector CD8 T cells to Tregs. D, $CD86^+$ cells as a percentage of NK1.1 cells. Graphs include values for individually analyzed mice, and the mean ± SEM of 9 mice per treatment group. One-way ANOVA was used to determine statistical significance (*, $P < 0.05$; **, $P < 0.01$; ***, $P < 0.001$). ns, not statistically significant.

PD-L1, and PD-L2, as well as combinations with predicted complementary benefit. Among mice with established intracranial tumors, we noted that single-agent PD-1 blockade achieved long-term survival among 50% of treated mice, whereas 15% to 20% of animals treated with CTLA-4 or PD-L1 mAbs alone were long-term survivors.

Long-term survivors in our study were effectively cured, as none of these animals showed evidence of viable tumor on histopathologic

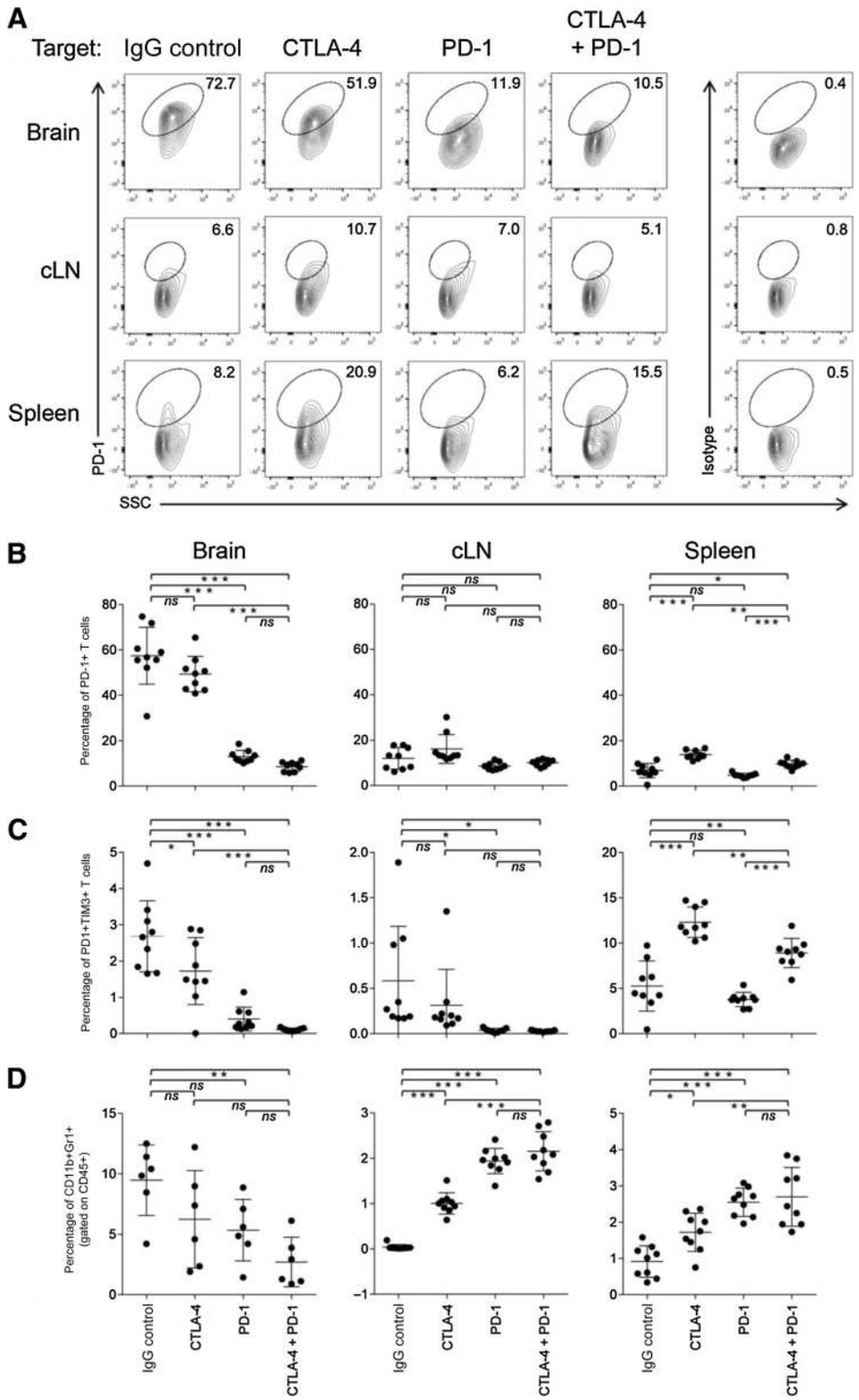

Figure 6.
Suppressive immune cell infiltrates within intracranial tumor, draining cervical lymph nodes (cLN), and spleen following checkpoint blockade. Mice were treated and cells prepared as in Fig. 5. A, expression of PD-1 on T cells gated for live $CD45^+CD3^+$ cells. Isotype control antibody staining is shown on the right. B and C, representative flow cytometry contour plots from each tissue of all treatment groups. Percentages of $CD45^+CD3^+$ T cells that are (B) $PD\text{-}1^+$ and (C) $PD\text{-}1^+/TIM3^+$. D, $CD11b^+/Gr1^+$ MDSCs as a percentage of live $CD45^+$ cells. Graphs include values for individually analyzed mice, and the mean ± SEM of 9 mice per treatment group. One-way ANOVA was used to determine statistical significance (*, $P < 0.05$; **, $P < 0.01$; ***, $P < 0.001$). ns, not statistically significant.

evaluation upon sacrifice. Although other groups have evaluated single-agent CTLA-4, PD-1, or PD-L1 blockade in glioblastoma models, evidence of antitumor benefit varied considerably. For example, CTLA-4 blockade achieves high (≥80%; refs. 14, 17), intermediate (20), or low/nonexistent (18, 19) rates of long-term survival. Similarly, blockade of either PD-1 or PD-L1 results in either high (20) or little (16) clinical benefit. The variability of therapeutic benefit observed across these studies likely reflects

differences in experimental design, such as choice of glioblastoma model, choice of blocking mAb, and timing/dosing of mAb administration. In contrast, a distinguishing feature of our study was that all of these variables were controlled, allowing consecutive experiments to specifically assess the relative impact of each immune checkpoint molecule. Of note, our experiments also uniquely evaluated PD-L2 blockade for glioblastoma, although the lack of observed therapeutic benefit may be due to absence of PD-L2 expression by GL261 (Supplementary Fig. S7). Nonetheless, our results suggest that single-agent immune checkpoint blockade should prioritize targeting PD-1 for clinical translation among patients with glioblastoma, although CTLA-4 and PD-L1 blockade also warrants clinical investigation.

Among combinatorial regimens, administration of CTLA-4 plus PD-1 mAb therapy was most active and resulted in marked increase in both the percentage of long-term survivors and median overall survival, compared with controls or monotherapy with either agent. Approximately 75% of animals treated with this combination were long-term, tumor-free survivors. These findings are consistent with a recent clinical trial that observed a 2- to 3-fold increase in durable responses among advanced melanoma patients treated with combined CTLA-4 and PD-1 mAb therapy compared with single-agent historical data, although higher rates of immune-related adverse events were noted with combined therapy (21). Our study is the only one to also evaluate combinatorial targeting of PD-1 plus PD-L1, as well as PD-L1 plus PD-L2, as strategies to more effectively block PD-1–mediated immunosuppression. We noted that these combinations offered no increased therapeutic benefit compared with single-agent therapy. Whether these results are applicable to other cancer models will require further study. In addition, we observed modestly increased benefit of CTLA-4 plus PD-L1 blockade as has been reported (20). Finally, in our experiments, there were no clinically apparent adverse events among responding mice treated with immune checkpoint blockade, including combinatorial therapy. Treated mice showed normal activity and did not develop weight loss or exhibit evidence of neurologic or hormonal deficits, although detailed, organ-specific, histopathologic, or laboratory examinations were not performed.

The reason for the greater efficacy of PD-1 blockade relative to PD-L1 or CTLA-4 in this glioblastoma model, as well as combinations thereof, remains to be determined, but several factors may contribute. First, the immunoinhibitory mechanisms of PD-1 and CTLA-4 are inherently distinct (21) and most active on distinct cells in different locations. Because B7 ligands are primarily expressed in lymphoid tissue, CTLA-4 blockade is thought to be most important in lymphoid organs, particularly on Tregs that express high levels of CTLA-4. In contrast, PD-1/PD-L1 interactions are thought to predominate in nonlymphoid tissues with PD-1 expression on $CD8^-$ T cells within the tumor microenvironment considered particularly important. In addition, PD-L1 expression in glioblastoma tumors may be upregulated by several factors, including IFNγ, VEGF, and oncogenic changes. We confirmed PD-L1 expression by GL-261, and a recent report demonstrates significant PD-L1 expression by most glioblastoma tumors (22). This expression pattern may mean that T cells can enter CNS tissue precoated with PD-1 mAb or require less PD-1 than PD-L1 mAb *in situ* for effective blockade. Finally, PD-L2 can inhibit T-cell activation and would be affected by PD-1 but not PD-L1 blockade. PD-1 blockade may therefore promote antitumor immune activity to a greater extent compared with CTLA-4 or PD-L1 inhibition. All of these factors may contribute to variable antitumor responses associated with administration of different immune checkpoint–blocking antibodies across tumor models and potentially between individually treated patients in the clinic.

In addition, we demonstrated that CTLA-4 or PD-1 mAb therapy alone and in combination was effective against advanced, later-stage, intracranial glioblastoma tumors. In fact, the percentage of long-term survivors among animals treated beginning 14 days after tumor implantation was comparable with that achieved when treatment was initiated 6 days after implantation. Successful treatment of late-stage tumors is of particular relevance to patients with glioblastoma, who are often confronted clinically with large, unresectable, and aggressively growing tumors. Based on our systematic evaluation of combinatorial regimens against both established and advanced glioblastoma models, our results support prioritizing combinatorial blockade of CTLA-4 plus PD-1 for clinical development among patients with glioblastoma, while combination treatment targeting CTLA-4 plus PD-L1 may also warrant clinical evaluation.

An exciting capability of immunotherapy is its ability to exert a dual-phase therapeutic benefit that initially includes effective treatment of existing tumors, followed by prevention of future relapse by successful induction of tumor-specific immune memory responses. Another strategic aspect of our experiments was demonstration that increased survival was also associated with evidence of tumor-specific immunologic memory. Specifically, intracranial rechallenge experiments revealed no evidence of tumor growth in all but one long-term surviving animal following initial CTLA-4, PD-1, or CTLA-4 plus PD-1 mAb combination therapy. Prior studies demonstrated induction of memory responses capable of rejecting flank tumor rechallenge (16, 18, 19); however, in our hands, tumors grew in only 50% of injected C57BL/6 mice who underwent flank injection of GL261-luc2, indicating that the flank may not be a reliable site to evaluate the induction of antitumor immune responses. In contrast, over 90% of mice developed tumors when either GL261 or GL261-luc2 was injected intracranially. Our study uniquely demonstrated that induced systemic immune memory responses are capable of rejecting tumor rechallenge in the CNS. The latter finding is particularly relevant to glioblastoma given that relapse universally occurs within the CNS and very rarely occurs systemically.

Another key aspect of our experiments was a detailed investigation of changes among immune cell populations within the glioblastoma microenvironment, draining cervical lymph nodes and the spleen, as well as changes in circulating immunocytokines. The degree of therapeutic benefit for single agent as well as combination immune checkpoint blockade was associated with reproducible changes in immune cell subsets. Changes in the brain and cervical lymph nodes showed a similar trend in most cases, whereas changes in the spleen were more variable. Treated tumors draining cervical lymph nodes had an increase in the infiltration of effector $CD8^+$ cells and activated NK cells. Simultaneously, the percentage of immunosuppressive lymphocytes, including Tregs, PD-1^+ lymphocytes, PD-1^+/TIM-3^+ exhausted T cells, and MDSCs, decreased. Our results are consistent with those from previous studies of checkpoint blockade (14, 16, 19, 20), and were marked in animals treated with combination CTLA-4 plus PD-1 mAb therapy. We also observed a systemic increase in several IFNγ-inducible chemokines, including CCL9 (MIP-1γ), CCL6 (C10), CCL11 (eotaxin), and CXCL12 (SDF-1).

In conclusion, we demonstrated that systemic administration of CTLA-4, PD-L1, and PD-1 inhibitors can improve survival for intracranial glioblastoma tumors. Single-agent blockade achieved durable survival benefit in a subset of tumor-bearing animals that was most robust with PD-1 mAb therapy, but dual blockade of CTLA-4 plus PD-1 exhibited the greatest antitumor benefit. CTLA-4 plus PD-L1 had modest activity, while PD-L1 with either PD-1 or PD-L2 revealed no additive benefit. Significant therapeutic benefit was achieved against advanced, later-stage tumors and was associated with specific systemic antitumor immunologic memory responses that prevented CNS relapse upon intracranial rechallenge. Mechanistically, tumor and cervical lymph node infiltration of effector immune cells was enhanced, and this activity is likely augmented by a concurrent decrease in immune cells capable of inhibiting antitumor responses in animals with improved survival. Our findings support the clinical evaluation of immune checkpoint blockade for patients with glioblastoma and prioritize targeting CTLA-4, PD-L1, and PD-1 separately and in combinatorial regimens for clinical development.

Disclosure of Potential Conflicts of Interest

D.A. Reardon has received honoraria for service on the speakers bureau for Bristol-Myers Squibb, Genentech, and Merck; and is a consultant/advisory board member for Bristol-Myers Squibb, Regeneron, and Roche. F.S. Hodi serves as a consultant for Genentech and Merck. A.H. Sharpe has served on advisory boards for CoStim and Surface Oncology and is a consultant for Novartis. She has patents/pending royalties from Roche and Novartis. G. Dranoff is Global Head of Exploratory Immune-Oncology at Novartis; reports receiving commercial research support from Bristol-Myers Squibb and Novartis; and is a consultant/advisory board member for Novartis. G.J. Freeman has served on advisory boards for CoStim, Novartis, Roche, and Bristol-Myers Squibb. He has patents/pending royalties with Bristol-Myers Squibb, Roche, Merck, EMD-Serono, Boehringer-Ingelheim, AstraZeneca, and Novartis. No potential conflicts of interest were disclosed by the other authors.

The founding Editor-in-Chief, Glenn Dranoff, is an author on this article. In keeping with the AACR's editorial policy, the peer review of this submission was managed by a senior member of *Cancer Immunology Research's* editorial team; a member of the AACR Publications Committee rendered the final decision concerning acceptability.

Authors' Contributions

Conception and design: D.A. Reardon, P.C. Gokhale, S.R. Klein, S.J. Rodig, A.D. Van Den Abbeele, G.J. Freeman

Development of methodology: D.A. Reardon, P.C. Gokhale, S.R. Klein, K.L. Ligon, S.J. Rodig, A.D. Van Den Abbeele, N.E. Kohl, G.J. Freeman

Acquisition of data (provided animals, acquired and managed patients, provided facilities, etc.): D.A. Reardon, P.C. Gokhale, S.R. Klein, K.L. Ligon, S.H. Ramkissoon, K.L. Jones, A.S. Conway, A.D. Van Den Abbeele, F.S. Hodi, L. Qin, N.E. Kohl, G.J. Freeman

Analysis and interpretation of data (e.g., statistical analysis, biostatistics, computational analysis): D.A. Reardon, P.C. Gokhale, S.R. Klein, K.L. Ligon, S.J. Rodig, S.H. Ramkissoon, K.L. Jones, X. Liao, A.D. Van Den Abbeele, F.S. Hodi, N.E. Kohl, A.H. Sharpe, G. Dranoff, G.J. Freeman

Writing, review, and/or revision of the manuscript: D.A. Reardon, P.C. Gokhale, S.R. Klein, K.L. Ligon, S.J. Rodig, S.H. Ramkissoon, J. Zhou, P.Y. Wen, A.D. Van Den Abbeele, F.S. Hodi, L. Qin, A.H. Sharpe, G. Dranoff, G.J. Freeman

Administrative, technical, or material support (i.e., reporting or organizing data, constructing databases): D.A. Reardon, P.C. Gokhale, K.L. Jones, A.S. Conway

Study supervision: D.A. Reardon, P.C. Gokhale, K.L. Ligon, A.D. Van Den Abbeele, N.E. Kohl, G.J. Freeman

Acknowledgments

The authors gratefully acknowledge the following organizations for funding support: The Ben and Catherine Ivy Foundation; Hope It's A Beach Thing; and the Rachel Molly Markoff Foundation.

Grant Support

NIH funding support was from NCI U54CA163125 and NCI P50 CA101942 (to A.S. Conway and G.J. Freeman).

The costs of publication of this article were defrayed in part by the payment of page charges. This article must therefore be hereby marked *advertisement* in accordance with 18 U.S.C. Section 1734 solely to indicate this fact.

Received June 23, 2015; revised September 24, 2015; accepted October 6, 2015; published OnlineFirst November 6, 2015.

References

1. Chinot OL, Wick W, Mason W, Henriksson R, Saran F, Nishikawa R, et al. Bevacizumab plus radiotherapy-temozolomide for newly diagnosed glioblastoma. N Engl J Med 2014;370:709–22.
2. Gilbert MR, Dignam JJ, Armstrong TS, Wefel JS, Blumenthal DT, Vogelbaum MA, et al. A randomized trial of bevacizumab for newly diagnosed glioblastoma. N Engl J Med 2014;370:699–708.
3. Stupp R, Hegi ME, Gorlia T, Erridge SC, Perry J, Hong YK, et al. Cilengitide combined with standard treatment for patients with newly diagnosed glioblastoma with methylated MGMT promoter (CENTRIC EORTC 26071-22072 study): a multicentre, randomised, open-label, phase 3 trial. Lancet Oncol 2014;15:1100–8.
4. Louveau A, Smirnov I, Keyes TJ, Eccles JD, Rouhani SJ, Peske JD, et al. Structural and functional features of central nervous system lymphatic vessels. Nature 2015;523:337–41.
5. Fecci PE, Heimberger AB, Sampson JH. Immunotherapy for primary brain tumors: no longer a matter of privilege. Clin Cancer Res 2014;20:5620–9.
6. Berghoff AS, Kiesel B, Widhalm G, Rajky O, Ricken G, Wohrer A, et al. Programmed death ligand 1 expression and tumor-infiltrating lymphocytes in glioblastoma. Neuro Oncol 2015;17:1064–75.
7. Akbari O, Stock P, Singh AK, Lombardi V, Lee WL, Freeman GJ, et al. PD-L1 and PD-L2 modulate airway inflammation and iNKT-cell-dependent airway hyperreactivity in opposing directions. Mucosal Immunol 2010;3:81–91.
8. Maes W, VanGool SW. Experimental immunotherapy for malignant glioma: lessons from two decades of research in the GL261 model. Cancer Immunol Immunother 2011;60:153–60.
9. Peng Y, Luo G, Zhou J, Wang X, Hu J, Cui Y, et al. CD86 is an activation receptor for NK cell cytotoxicity against tumor cells. PLoS One 2013;8:e83913.
10. Hanna J, Fitchett J, Rowe T, Daniels M, Heller M, Gonen-Gross T, et al. Proteomic analysis of human natural killer cells: insights on new potential NK immune functions. Mol Immunol 2005;42:425–31.
11. Sakuishi K, Apetoh L, Sullivan JM, Blazar BR, Kuchroo VK, Anderson AC. Targeting Tim-3 and PD-1 pathways to reverse T cell exhaustion and restore anti-tumor immunity. J Exp Med 2010;207:2187–94.
12. Fourcade J, Sun Z, Benallaoua M, Guillaume P, Luescher IF, Sander C, et al. Upregulation of Tim-3 and PD-1 expression is associated with tumor antigen-specific CD8+ T cell dysfunction in melanoma patients. J Exp Med 2010;207:2175–86.
13. Wang C, Thudium KB, Han M, Wang XT, Huang H, Feingersh D, et al. In vitro characterization of the anti-PD-1 antibody nivolumab, BMS-936558, and in vivo toxicology in non-human primates. Cancer Immunol Res 2014;2:846–56.
14. Fecci PE, Ochiai H, Mitchell DA, Grossi PM, Sweeney AE, Archer GE, et al. Systemic CTLA-4 blockade ameliorates glioma-induced changes to the CD4+ T cell compartment without affecting regulatory T-cell function. Clin Cancer Res 2007;13:2158–67.
15. Wainwright DA, Balyasnikova IV, Chang AL, Ahmed AU, Moon KS, Auffinger B, et al. IDO expression in brain tumors increases the recruitment of regulatory T cells and negatively impacts survival. Clin Cancer Res 2012;18:6110–21.

16. Zeng J, See AP, Phallen J, Jackson CM, Belcaid Z, Ruzevick J, et al. Anti-PD-1 blockade and stereotactic radiation produce long-term survival in mice with intracranial gliomas. Int J Radiat Oncol Biol Phys 2013;86:343–9.
17. Agarwalla P, Barnard Z, Fecci P, Dranoff G, Curry WT, Jr. Sequential immunotherapy by vaccination with GM-CSF-expressing glioma cells and CTLA-4 blockade effectively treats established murine intracranial tumors. J Immunother 2012;35:385–9.
18. Vom Berg J, Vrohlings M, Haller S, Haimovici A, Kulig P, Sledzinska A, et al. Intratumoral IL-12 combined with CTLA-4 blockade elicits T cell-mediated glioma rejection. J Exp Med 2013;210:2803–11.
19. Belcaid Z, Phallen JA, Zeng J, See AP, Mathios D, Gottschalk C, et al. Focal radiation therapy combined with 4-1BB activation and CTLA-4 blockade yields long-term survival and a protective antigen-specific memory response in a murine glioma model. PLoS One 2014;9: e101764.
20. Wainwright DA, Chang AL, Dey M, Balyasnikova IV, Kim CK, Tobias A, et al. Durable therapeutic efficacy utilizing combinatorial blockade against IDO, CTLA-4, and PD-L1 in mice with brain tumors. Clin Cancer Res 2014; 20:5290–301.
21. Sharma P, Allison JP. The future of immune checkpoint therapy. Science 2015;348:56–61.
22. Berghoff AS, Kiesel B, Widhalm G, Rajky O, Ricken G, Wohrer A, et al. Programmed death ligand 1 expression and tumor-infiltrating lymphocytes in glioblastoma. Neuro Oncol 2015;17:1064–75.